Computers, Materials & Continua
DOI:10.32604/cmc.2022.020384
Article

Tech Science Press

A Study of Cellular Neural Networks with Vertex-Edge Topological Descriptors

Sadia Husain[1], Muhammad Imran[2,*], Ali Ahmad[1], Yasir Ahmad[1] and Kashif Elahi[3]

[1]Country College of Computer Science & Information Technology, Jazan University, Jazan, Saudi Arabia
[2]Department of Mathematical Sciences, United Arab Emirates University, Al Ain, United Arab Emirates
[3]Deanship of E-learning and Information Technology, Jazan University, Jazan, Saudi Arabia
[*]Corresponding Author: Muhammad Imran. Email: imrandhab@gmail.com
Received: 22 May 2021; Accepted: 23 June 2021

Abstract: The Cellular Neural Network (CNN) has various parallel processing applications, image processing, non-linear processing, geometric maps, high-speed computations. It is an analog paradigm, consists of an array of cells that are interconnected locally. Cells can be arranged in different configurations. Each cell has an input, a state, and an output. The cellular neural network allows cells to communicate with the neighbor cells only. It can be represented graphically; cells will represent by vertices and their interconnections will represent by edges. In chemical graph theory, topological descriptors are used to study graph structure and their biological activities. It is a single value that characterizes the whole graph. In this article, the vertex-edge topological descriptors have been calculated for cellular neural network. Results can be used for cellular neural network of any size. This will enhance the applications of cellular neural network in image processing, solving partial differential equations, analyzing 3D surfaces, sensory-motor organs, and modeling biological vision.

Keywords: Cellular neural networks; degree; topological indices

1 Introduction

Graph theory is a vast field and is used to solve real problems and natural phenomena. That's why it has applications in molecular chemistry, robotics, physics, networks, computer science, statistics, biological activities, and data science. It represents real scenarios in the graph based on vertices and edges.

A topological descriptor is a single value that characterizes the whole graph [1–3]. In chemical graph theory, they are used to estimate biological activities and atomic movements [4–6]. The first topological descriptor Wiener index was introduced by Wiener in 1947 [7]. Hosoya polynomial, Schultz index, atom bond connectivity, geometric-arithmetic index are other famous topological descriptors [4,8,9]. Topological descriptors can be categorized on the basis of the mechanism of calculation involved [10–17]. Nowadays vertex-edge topological descriptors are gaining importance in applied sciences [18].

Let G be a simple connected graph with vertex sets $V(G)$ and edge sets $E(G)$. The degree of a vertex ϵ, denoted by $d(\epsilon)$, is the number of edges that are incident to the ϵ. The open neighbourhood of ϵ is defined as $N(\epsilon) = \{\varepsilon \in V(G) : \epsilon\varepsilon \in E(G)\}$ and closed neighbourhood $N[\epsilon] = N(\epsilon) \cup \{\epsilon\}$ [19]. The *ve*-degree, denoted by $d_{ve}(\epsilon)$, of any vertex $\epsilon \in V$ is the number of different edges that are incident to any vertex from the $N[\epsilon]$. In [20] defined the *ev*-degree of the edge $e = \epsilon\varepsilon \in E$, denoted by $d_{ev}(e)$, the number of vertices of the union of the closed neighborhoods of ϵ and ε. For details see [21–27].

The *ve*-degree and *ev*-degree topological indices are defined as: $\sum_{e\in E(G)} (d_{ev}(e))^2$, $\sum_{\epsilon\in V} d_{ve}(\epsilon)^2, \sum_{\epsilon\varepsilon\in E} (d_{ve}(\epsilon) + d_{ve}(\varepsilon))$, $\sum_{\epsilon\varepsilon\in E} (d_{ve}(\epsilon) \times d_{ve}(\varepsilon))$, $\sum_{\epsilon\varepsilon\in E} (d_{ve}(\epsilon) \times d_{ve}(\epsilon))^{-\frac{1}{2}}$, $\sum_{e_1 E} d_{ve}(e_1)^{-\frac{1}{2}}$, $\sum_{\epsilon\varepsilon\in E} \left(\frac{d_{ve}(\epsilon)+d_{ve}(\varepsilon)-2}{d_{ve}(\epsilon)\times d_{ve}(\varepsilon)}\right)^{\frac{1}{2}}$, $\sum_{\epsilon\varepsilon\in E} \frac{2(d_{ve}(\epsilon)\times d_{ve}(\varepsilon))^{\frac{1}{2}}}{d_{ve}(\epsilon)+d_{ve}(\varepsilon)}$, $\sum_{\epsilon\varepsilon\in E} \frac{2}{d_{ve}(\epsilon)+d_{ve}(\varepsilon)}$ and $\sum_{\epsilon\varepsilon\in E} (d_{ve}(\epsilon) + d_{ve}(\varepsilon))^{-\frac{1}{2}}$ are named as: *ev*-degree Zagreb (M_{ev}) index, the first *ve*-degree Zagreb α ($M^1_{\alpha ve}$) index, the first *ve*-degree Zagreb β ($M^1_{\beta ve}$) index, the second *ve*-degree Zagreb (M^2_{ve}) index, *ve*-degree Randic (R_{ve}) index, the *ev*-degree Randic (R_{ev}) index, the *ve*-degree atom-bond connectivity (ABC_{ve}) index, the *ve*-degree geometric-arithmetic (GA_{ve}) index, the *ve*-degree harmonic (H_{ve}) index and the *ve*-degree sum-connectivity (χ_{ve}) index, respectively.

2 Applications and Importance

The Cellular Neural Network (CNN) is an array of cells that are interconnected locally. It is an analog paradigm with various applications including image processing, parallel processing, and high-speed computations. Each cell has an input, an output, and its state. A cell can interact with neighbor cells only. A neighbor cell of a cell is in its radius. A neighborhood includes the cell itself and its eight neighboring cells [28,29]. Fig. 1, consists of two diagrams (a) and (b). Diagram (a), is a graph of two-dimensional CNN, in which a neighborhood is representing red and blue colors. Diagram (b), is the internal structure of the red cell of diagram (a), this cell can interact with all blue cells in this neighborhood. In this article, vertex-edge topological descriptors have been calculated for CNN. The results are generalized and can be used for CNN of any structure and size. This will enhance the applications of CNN in image processing, parallel processing, image processing, non-linear processing, geometric maps, high-speed computations, solving partial differential equations, analyzing 3D surfaces, sensory-motor organs, and modeling biological vision [30].

In 2018, new degree-based topological indices are considered and the analytical sharp bounds has been derived for neural networks in [31]. In 2019, Imran et al. [32] has been calculated the degree based topological indices of cellular neural network. Topology optimization and Zagreb connection indices for cellular neural network are studied in [30,33]. Recently in 2021, the comparison and analysis between the dominating topological indices are determined for the cellular neural network [34]. Some topological indices have been calculated for cellular neural network, and are prominence their importance, but still many topological indices have not been calculated. Their calculation will provide an analytical study of cellular neural network in different applications. The cellular neural network is also known as the strong product of two paths, which has applications in different area of research, see [35,36].

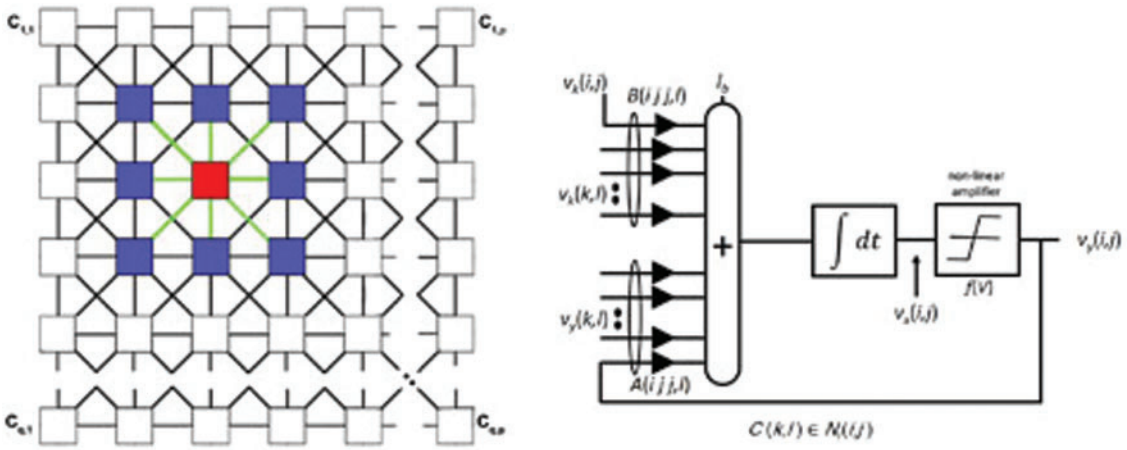

Figure 1: Graph of cellular neural networks. (a) Two-dimensional CNN graph, (b) red cell internal structure of (a)

3 The Graph of Cellular Neural Networks

The Figs. 2 and 3 show cellular neural network for different values of p and q.

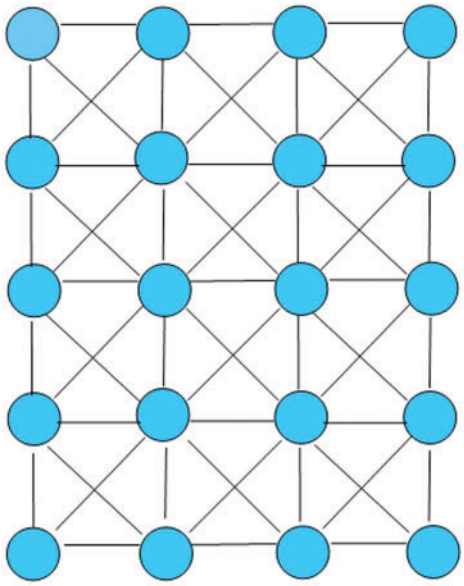

Figure 2: Graph representing cellular neural networks p = 5 (rows) and q = 4 (columns)

The cellular neural network can be arranged either linearly or in a sheet form. A cellular neural network of p rows and q columns, contains pq vertices and $4pq-3p-3q+2$ edges, which are shown in Tab. 1. The number of vertices corresponding to their degrees of CNN are shown in Tab. 2 and the edge partition based on degree of end vertices of each edge is shown in the Tab. 3.

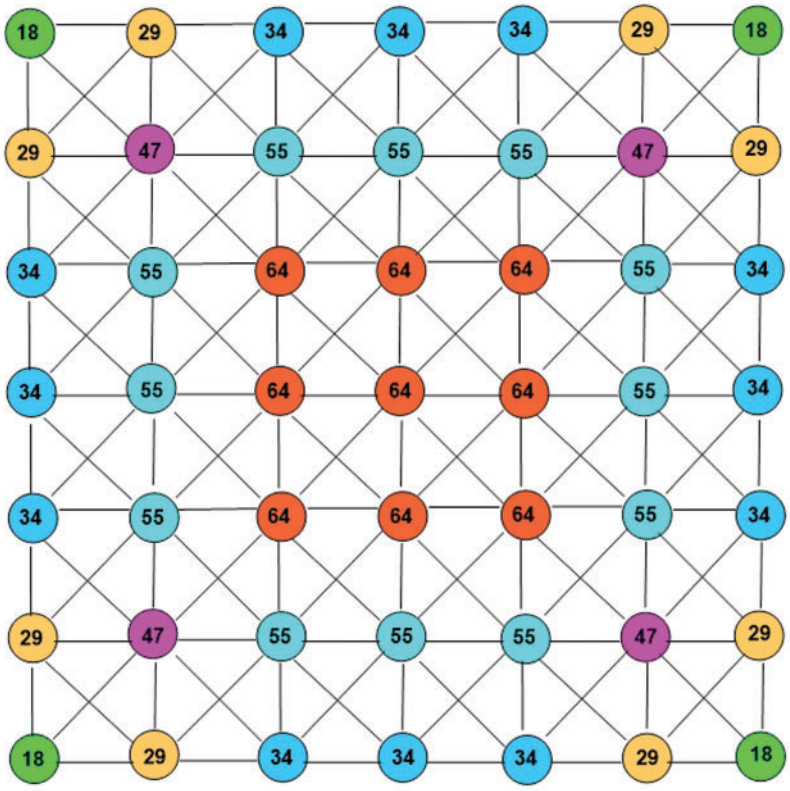

Figure 3: This is an example of cellular neural networks graph for p = 7 and q = 7 along with sum of degrees of neighborhood vertices

Table 1: Vertices and edges of CNN

Total vertices	Total edges
pq	$4pq-3p-3q+2$

Table 2: Number of vertices corresponding to their degrees of CNN

$d(\epsilon)$	Number of vertices
3	4
5	8
5	$2(p+q)-16$
8	4
8	$2(p+q)-16$
8	$(p-4)(q-4)$
Total	pq

We partitioned the edges of CNN, based on *ev*-degree in Tab. 4.

In Tab. 5, we partitioned the vertices of CNN, based on *ev*-degree.

Table 3: Edge partition of CNN

$(d(\epsilon), d(\varepsilon))$	Number of edges
(3, 5)	8
(3, 8)	4
(5, 5)	$2(p+q-4)$
(5, 8)	$6(p+q)-32$
(8, 8)	$4pq-11(p+q)+30$
Total	$4pq-3p-3q+2$

Table 4: Edge partition of CNN

Number of edges	$d_{ev}(\epsilon)$	$(d(\epsilon), d(\varepsilon))$
8	8	(3, 5)
4	11	(3, 8)
$2(p+q-4)$	10	(5, 5)
$6(p+q)-32$	13	(5, 8)
$4pq-11(p+q)+30$	16	(8, 8)

Table 5: Vertex partition of CNN, based on ve-degree

Number of vertices	$d_{ve}(\epsilon)$	$d(\epsilon)$
4	18	3
8	29	5
$2(p+q)-16$	34	5
4	47	8
$2(p+q)-16$	55	8
$(p-4)(q-4)$	64	8

We partitioned the edge of CNN with respect to *ve*-degrees.

Now we calculated *ev*-degree and *ve*-degree based indices such as M_{ev} index, $M^1_{\alpha ve}$ index, $M^1_{\beta ve}$ index, M^2_{ve} index, R_{ve} index, R_{ev} index, ABC_{ve} index, GA_{ve} index, H_{ve} index and χ_{ve} index for CNN.

3.1 The ev-Degree Zagreb Index

The values of *ev*-degree of each edge is calculated by the sum of degree of its end vertices. The edge partition according to *ev*-degree for cellular neural network (CNN) is shown in Tab. 4. By using *ev*-degree of *CNN* from Tab. 4, we compute the *ev*-degree based Zagreb index:

$$\begin{aligned} M^{ev}(CNN) &= \sum_{e\in E(CNN)} (d_{ev}(e))^2 \\ &= 8\times 8^2 + 4\times 11^2 + (2p+2q-8)\times 10^2 + (6p+6q-32)\times 13^2 \\ &\quad + (4pq-11p-11q+30)\times 16^2 \\ &= 1024pq - 1602p - 1602q + 2468. \end{aligned}$$

3.2 The First ve-Degree Zagreb α Index

The *ve*-degree of each vertex is obtained by the sum of all degrees of its neighboring vertices. We partitioned the vertices of cellular neural network (CNN) according to its *ve*-degree that is shown in Tab. 5. Using Tab. 5 we compute the first *ve*-degree Zagreb α index:

$$M^1_{\alpha ve}(CNN) = \sum_{\epsilon \in V} d_{ve}(\epsilon)^2$$

$$\begin{aligned} M^1_{\alpha ve}(CNN) &= 4 \times 18^2 + 8 \times 29^2 + (2q + 2p - 16) \times 34^2 + 4 \times 47^2 + (2q + 2p - 16) \times 55^2 \\ &\quad + (pq - 4q - 4p + 16) \times 64^2 \\ &= 4096pq - 8022(p + q) + 15500. \end{aligned}$$

3.3 The First ve-Degree Zagreb β Index

The edge partition of cellular neural network (CNN) with respect to *ve*-degree is shown in Tab. 6. Using Tab. 6 we compute the first *ve*-degree Zagreb β index:

$$M^1_{\beta ve}(CNN) = \sum_{\epsilon\varepsilon \in E} (d_{ve}(\epsilon) + d_{ve}(\varepsilon))$$

$$\begin{aligned} M^1_{\beta ve}(CNN) &= 8 \times (18 + 29) + 4 \times (18 + 47) + 4 \times (29 + 29) + 8 \times (29 + 34) + (2p + 2q - 20) \\ &\quad \times (34 + 34) + 8 \times (29 + 47) + 8 \times (29 + 55) + 8 \times (34 + 47) + (6p + 6q - 56) \\ &\quad \times (34 + 55) + 8 \times (47 + 55) + 4 \times (47 + 64) + (2p + 2q - 16) \times (55 + 55) + (6p + 6q - 56) \\ &\quad \times (55 + 64) + (2pq - 8p - 8q + 32) \times (64 + 64) \\ &= 256pq + 580(p + q) - 6112. \end{aligned}$$

Table 6: Edge partition of CNN, based on ve-degree

Number of edges	$(d_{ve}(\epsilon), d_{ve}(\varepsilon))$	$(d(\epsilon), d(\varepsilon))$
8	(18, 29)	(3, 5)
4	(18, 47)	(3, 8)
4	(29, 29)	(5, 5)
8	(29, 34)	(5, 5)
$2(p-5)+2(q-5)$	(34, 34)	(5, 5)
8	(29, 47)	(5, 8)
8	(29, 55)	(5, 8)
8	(34, 47)	(5, 8)
$2(3p-14)+2(3q-14)$	(34, 55)	(5, 8)
8	(47, 55)	(8, 8)
4	(47, 64)	(8, 8)
$2(p+q-8)$	(55, 55)	(8, 8)
$6(p-6)+6(q-6)+16$	(55, 64)	(8, 8)
$2(p-4)(q-4)$	(64, 64)	(8, 8)

3.4 The Second ve-Degree Zagreb Index

Using Tab. 6 we compute the second *ve*-degree Zagreb index:

$$M_{ve}^{2}(CNN)=\sum_{\epsilon\varepsilon\in E}\left(d_{ve}(\epsilon)\times d_{ve}(\varepsilon)\right)$$

$$\begin{aligned}M_{ve}^{2}(CNN)&=8\times(18\times29)+4\times(18\times47)+4\times(29\times29)+8\times(29\times34)+(2p+2q-20)\times(34\times34)\\&\quad+8\times(29\times47)+8\times(29\times55)+8\times(34\times47)+(6p+6q-56)\times(34\times55)\\&\quad+8\times(47\times55)+4\times(47\times64)+(2p+2q-16)\times(55\times55)+(6p+6q-56)\\&\quad\times(55\times64)+(2pq-8p-8q+32)\times(64\times64)\\&=8192pq+7934(p+q)-154316.\end{aligned}$$

3.5 The ve-Degree Randic Index

Using Tab. 6 we compute the *ve*-degree Randic index:

$$R_{ve}(CNN)=\sum_{\epsilon\varepsilon\in E}\left(d_{ve}(\epsilon)\times d_{ve}(\epsilon)\right)^{-\frac{1}{2}}$$

$$\begin{aligned}R_{ve}(CNN)&=8\times(18\times29)^{-\frac{1}{2}}+4\times(18\times47)^{-\frac{1}{2}}+4\times(29\times29)^{-\frac{1}{2}}+8\times(29\times34)^{-\frac{1}{2}}+(2p+2q-20)\\&\quad\times(34\times34)^{-\frac{1}{2}}+8\times(29\times47)^{-\frac{1}{2}}+8\times(29\times55)^{-\frac{1}{2}}+8\times(34\times47)^{-\frac{1}{2}}+(6p+6q-56)\\&\quad\times(34\times55)^{-\frac{1}{2}}+8\times(47\times55)^{-\frac{1}{2}}+4\times(47\times64)^{-\frac{1}{2}}+(2p+2q-16)\times(55\times55)^{-\frac{1}{2}}\\&\quad+(6p+6q-56)\times(55\times64)^{-\frac{1}{2}}+(2pq-8p-8q+32)\times(64\times64)^{-\frac{1}{2}}\\&=\frac{4}{87}\sqrt{58}+\frac{2}{141}\sqrt{94}-\frac{13081}{54230}+\frac{4}{493}\sqrt{986}-\frac{223}{7480}p-\frac{223}{7480}q+\frac{8}{1363}\sqrt{1363}\\&\quad+\frac{8}{1595}\sqrt{1595}+\frac{4}{799}\sqrt{1598}+\frac{1}{1870}(6p+6q-56)\sqrt{1870}+\frac{8}{2585}\sqrt{2585}+\frac{1}{94}\sqrt{47}\\&\quad+\frac{1}{440}(6p+6q-56)\sqrt{55}+\frac{1}{32}pq\\&=\frac{1}{32}pq+\left(\frac{3}{935}\sqrt{1870}-\frac{223}{7480}+\frac{3}{220}\sqrt{55}\right)(p+q)+\frac{4}{87}\sqrt{58}+\frac{2}{141}\sqrt{94}-\frac{13081}{54230}+\frac{4}{493}\sqrt{986}\\&\quad+\frac{4}{799}\sqrt{1598}-\frac{28}{935}\sqrt{1870}+\frac{8}{1363}\sqrt{1363}+\frac{8}{1595}\sqrt{1595}+\frac{1}{94}\sqrt{47}+\frac{8}{2585}\sqrt{2585}-\frac{7}{55}\sqrt{55}.\end{aligned}$$

3.6 The ev-Degree Randic Index

Using Tab. 4 we compute the *ev*-degree Randic index:

$$R_{ev}(CNN)=\sum_{e_1E}d_{ev}(e_1)^{-\frac{1}{2}}$$

$$R_{ev}(CNN) = 8\times(8)^{-\frac{1}{2}} + 4\times(11)^{-\frac{1}{2}} + (2p+2q-8)\times(10)^{-\frac{1}{2}} + (6p+6q-32)\times(13)^{-\frac{1}{2}}$$
$$+ (4pq-11p-11q+30)\times(16)^{-\frac{1}{2}}$$
$$= 2\sqrt{2} + \frac{4}{11}\sqrt{11} + \frac{1}{10}(2p+2q-8)\sqrt{10} + \frac{1}{13}(6p+6q-32)\sqrt{13} + pq - \frac{11}{4}p - \frac{11}{4}q + \frac{15}{2}$$
$$= pq + \left(\frac{1}{5}\sqrt{10} - \frac{11}{4} + \frac{6}{13}\sqrt{13}\right)(p+q) + 2\sqrt{2} + \frac{4}{11}\sqrt{11} - \frac{4}{5}\sqrt{10} - \frac{32}{13}\sqrt{13} + \frac{15}{2}.$$

3.7 The ve-Degree Atom-Bond Connectivity Index

Using Tab. 6 we compute the *ve*-degree atom-bond connectivity index:

$$ABC_{ve}(CNN) = \sum_{\epsilon\varepsilon\in E}\left(\frac{d_{ve}(\epsilon) + d_{ve}(\varepsilon) - 2}{d_{ve}(\epsilon)\times d_{ve}(\varepsilon)}\right)^{\frac{1}{2}}$$

$$ABC_{ve}(CNN) = 8\times\sqrt{\frac{45}{522}} + 4\times\sqrt{\frac{63}{846}} + 4\times\sqrt{\frac{56}{841}} + 8\times\sqrt{\frac{61}{986}} + (2p+2q-20)\times\sqrt{\frac{66}{1156}}$$
$$+ 8\times\sqrt{\frac{74}{1363}} + 8\times\sqrt{\frac{82}{1595}} + 8\times\sqrt{\frac{79}{1598}} + (6p+6q-56)\times\sqrt{\frac{87}{1870}} + 8\times\sqrt{\frac{100}{2585}}$$
$$+ 4\times\sqrt{\frac{109}{3008}} + (2p+2q-16)\times\sqrt{\frac{108}{3025}} + (6p+6q-56)\times\sqrt{\frac{117}{3520}} + (2pq-8p$$
$$- 8q+32)\times\sqrt{\frac{126}{4096}}$$
$$= \frac{3}{32}\sqrt{14}pq + \left(\frac{3}{935}\sqrt{162690} + \frac{12}{55}\sqrt{3} + \frac{9}{220}\sqrt{715} + \frac{1}{17}\sqrt{66} - \frac{3}{8}\sqrt{14}\right)(p+q) + \frac{4}{29}\sqrt{290}$$
$$+ \frac{2}{47}\sqrt{658} + \frac{103}{58}\sqrt{14} + \frac{4}{493}\sqrt{60146} - \frac{10}{17}\sqrt{66} + \frac{8}{1595}\sqrt{130790} - \frac{28}{935}\sqrt{162690}$$
$$- \frac{96}{55}\sqrt{3} + \frac{8}{1363}\sqrt{100862} + \frac{16}{517}\sqrt{2585} + \frac{4}{799}\sqrt{126242} - \frac{21}{55}\sqrt{715} + \frac{1}{94}\sqrt{5123}.$$

3.8 The ve-Degree Geometric-Arithmetic Index

Using Tab. 6 we compute the *ve*-degree geometric-arithmetic index:

$$GA_{ve}(CNN) = \sum_{\epsilon\varepsilon\in E}\frac{2\left(d_{ve}(\epsilon)\times d_{ve}(\varepsilon)\right)^{\frac{1}{2}}}{d_{ve}(\epsilon) + d_{ve}(\varepsilon)}$$

$$GA_{ve}(CNN) = \frac{16\sqrt{522}}{47} + \frac{8\sqrt{846}}{65} + \frac{8\sqrt{841}}{58} + \frac{16\sqrt{986}}{63} + \frac{2(2p+2q-20)\sqrt{1156}}{68} + \frac{16\sqrt{1363}}{76}$$
$$+ \frac{16\sqrt{1595}}{84} + \frac{16\sqrt{1598}}{81} + \frac{2(6p+6q-56)\sqrt{1870}}{89} + \frac{16\sqrt{2585}}{102} + \frac{8\sqrt{3008}}{111}$$
$$+ \frac{2(2p+2q-16)\sqrt{3025}}{110} + \frac{2(6p+6q-56)\sqrt{3520}}{119} + \frac{2(2pq-8p-8q+32)\sqrt{4096}}{128}$$
$$= 2pq + \left(\frac{12}{89}\sqrt{1870} - 4 + \frac{96}{119}\sqrt{55}\right)(p+q) + \frac{48}{47}\sqrt{58} + \frac{24}{65}\sqrt{94} + \frac{16}{63}\sqrt{986} + \frac{16}{81}\sqrt{1598}$$
$$- \frac{112}{89}\sqrt{1870} + \frac{4}{19}\sqrt{1363} + \frac{4}{21}\sqrt{1595} + \frac{64}{111}\sqrt{47} + \frac{8}{51}\sqrt{2585} - \frac{128}{17}\sqrt{55}.$$

3.9 The ve-Degree Harmonic Index

Using Tab. 6 we compute the *ve*-degree harmonic index:

$$H_{ve}(CNN) = \sum_{\epsilon\varepsilon\in E} \frac{2}{d_{ve}(\epsilon) + d_{ve}(\varepsilon)}$$

$$H_{ve}(CNN) = \frac{16}{47} + \frac{8}{65} + \frac{8}{58} + \frac{16}{63} + \frac{2(2p+2q-20)}{68} + \frac{16}{76} + \frac{16}{84} + \frac{16}{81} + \frac{2(6p+6q-56)}{89} + \frac{16}{102}$$
$$+ \frac{8}{111} + \frac{2(2p+2q-16)}{110} + \frac{2(6p+6q-56)}{119} + \frac{2(2pq-8p-8q+32)}{128}$$
$$= \frac{1}{32}pq + \frac{959311}{4660040}p + \frac{959311}{4660040}q - \frac{30087768559241}{33584675843862}.$$

3.10 The ve-Degree Sum-Connectivity Index

Using Tab. 6 we compute the *ve*-degree sum-connectivity index:

$$\chi_{ve}(CNN) = \sum_{\epsilon\varepsilon\in E} (d_{ve}(\epsilon) + d_{ve}(\varepsilon))^{-\frac{1}{2}}$$

$$\chi_{ve}(CNN) = 8(47)^{-\frac{1}{2}} + 4(65)^{-\frac{1}{2}} + 4(58)^{-\frac{1}{2}} + 8(63)^{-\frac{1}{2}} + (2p+2q-20)(68)^{-\frac{1}{2}} + 8(76)^{-\frac{1}{2}} + 8(84)^{-\frac{1}{2}}$$
$$+ 8(81)^{-\frac{1}{2}} + (6p+6q-56)(89)^{-\frac{1}{2}} + 8(102)^{-\frac{1}{2}} + 4(111)^{-\frac{1}{2}} + (2p+2q-16)(110)^{-\frac{1}{2}}$$
$$+ (6p+6q-56)(119)^{-\frac{1}{2}} + (2pq-8p-8q+32)(128)^{-\frac{1}{2}}$$
$$= \frac{\sqrt{2}}{8}pq + \left(\frac{6}{89}\sqrt{89} + \frac{1}{55}\sqrt{110} + \frac{6}{119}\sqrt{119} + 1/17\sqrt{17}) - 1/2\sqrt{2}\right)(p+q) + \frac{8}{47}\sqrt{47} + \frac{4}{65}\sqrt{65}$$

$$+\frac{2}{29}\sqrt{58}+\frac{8}{21}\sqrt{7}-\frac{10}{17}\sqrt{17}+\frac{4}{21}\sqrt{21}-\frac{56}{89}\sqrt{89}-\frac{8}{55}\sqrt{110}+\frac{4}{19}\sqrt{19}+\frac{4}{51}\sqrt{102}+\frac{8}{9}$$
$$+2\sqrt{2}-\frac{8}{17}\sqrt{119}+\frac{4}{111}\sqrt{111}.$$

4 Numerical and Graphical Representation

In this section, we determine the numerical values of the $M^1_{\alpha ve}, M^1_{\beta ve}, M^2_{ve}, R_{ev}, ABC_{ve}, GA_{ve}, R_{ve}, H_{ve}, \chi_{ve}$, in Tabs. 7–9. We represented these results graphically in Figs. 4–6.

Table 7: Numerical comparison of $\boldsymbol{M^1_{\alpha ve}, M^1_{\beta ve}}$ and $\boldsymbol{M^2_{ve}}$

[p, q]	$M^1_{\alpha ve}$	$M^1_{\beta ve}$	M^2_{ve}
[5, 5]	12304	6088	129824
[6, 6]	20364	10064	235804
[7, 7]	30472	14552	358168
[8, 8]	42628	19552	496916
[9, 9]	56832	25064	652048
[10, 10]	73084	31088	823564
[11, 11]	91384	37624	1011464
[12, 12]	111732	44672	1215748
[13, 13]	134128	52232	1436416
[14, 14]	158572	60304	1673468

Table 8: Numerical comparison of $\boldsymbol{R_{ev}, ABC_{ve}}$ and $\boldsymbol{GA_{ve}}$

[p, q]	R_{ev}	ABC_{ve}	GA_{ve}
[5, 5]	20.595	16.952	72.413
[6, 6]	30.688	24.492	110.04
[7, 7]	42.781	32.733	151.67
[8, 8]	56.875	41.676	197.30
[9, 9]	72.968	51.322	246.92
[10, 10]	91.060	61.670	300.55
[11, 11]	111.15	72.718	358.17
[12, 12]	133.25	84.465	419.80
[13, 13]	157.34	96.917	485.43
[14, 14]	183.44	110.07	555.06

Table 9: Numerical comparison of R_{ve}, H_{ve} and χ_{ve}

[p, q]	R_{ve}	H_{ve}	χ_{ve}
[5, 5]	1.9915	1.9440	8.3964
[6, 6]	2.7556	2.6994	12.165
[7, 7]	3.5818	3.5174	16.288
[8, 8]	4.4709	4.3979	20.763
[9, 9]	5.4222	5.3408	25.593
[10, 10]	6.4360	6.3463	30.776
[11, 11]	7.5125	7.4143	36.313
[12, 12]	8.6513	8.5447	42.203
[13, 13]	9.8528	9.7377	48.446
[14, 14]	11.117	10.993	55.044

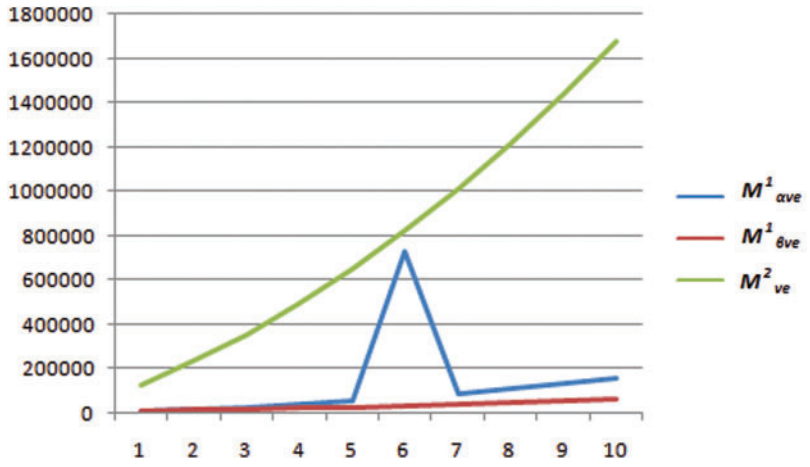

Figure 4: Graphical comparison of $M^1_{\alpha ve}, M^1_{\beta ve}$ and M^2_{ve} for CNN

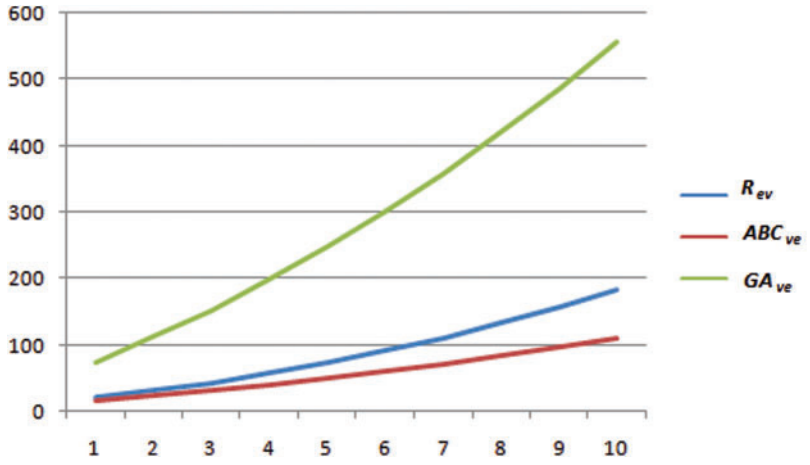

Figure 5: Graphical comparison of R_{ev}, ABC_{ve} and GA_{ve} for CNN

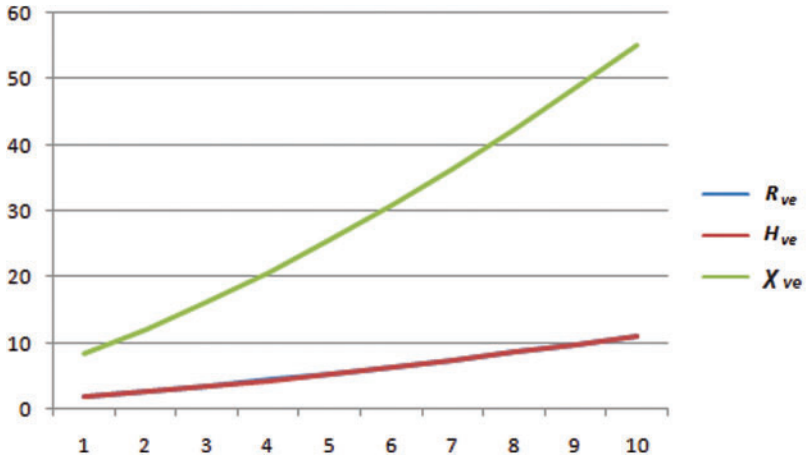

Figure 6: Graphical comparison of R_{ve}, H_{ve} and χ_{ve} for CNN

5 Advantages and Limitations

5.1 Advantages

As a machine learning algorithm, CNN can take image as an input, highlight image key features, and differentiate one image from the other [37]. CNN has powerful function-fitting capabilities and has great potential to study partial differential equations [38,39]. CNN has been widely used in analyzing 3D surfaces and facial images applications [40]. The design components underlying the implementation of the physiologically faithful retina and other topographic sensory organ models on CNN universal chips. The results obtained through the proposed technique can better understand the features and characteristics of CNN. It can enhance image processing applications, solve partial differential equations, analyze 3D surfaces, sensory-motor organs, and model biological vision. Combinations of CNN and artificial intelligence provide enhanced human-level performance to computer architectures [41]. This article is vital in the implementation of Human-level visual recognition.

5.2 Limitations

The calculation of vertex-edge topological descriptors carried out in this research are specifically derived for cellular neural networks. However, with some modifications they can be applied in other fields like image processing, biological modelling, 3D surface analyzing, and complex imaging. The applicability of this research still needs to be validated for these fields to identify the full potential of this research. These open problems can be further studied to get full benefit of this research.

6 Conclusion

A cell in Cellular Neural Network (CNN), can communicate with neighbor cells only. Due to its architecture, it is used to manage hierarchical levels, and it has variety of applications. In applied sciences, graph theory provides different tools and methods to remedy real-world problems. To solve these problems, it represents them in the form of graphs. Topological descriptors in graph theory are used to study and characterize biological activities in the form of graphs. In this article, the vertex-edge topological descriptors have been calculated for the graphic representation of CNN. Results can be used for the CNN of any size. The proposed technique can enhance the CNN's applications in image processing, parallel processing, non-linear processing, geometric

maps representations, high-speed computations, solving partial differential equations, analyzing 3D surfaces, sensory-motor organs, and modeling biological vision.

Funding Statement: This research is supported by the University program of Advanced Research (UPAR) and UAEU-AUA grants of United Arab Emirates University (UAEU) via Grant No. G00003271 and Grant No. G00003461.

Conflicts of Interest: The authors declare that they have no conflicts of interest to report regarding the present study.

References

[1] A. Ahmad, "On the degree based topological indices of benzene ring embedded in P-type-surface in 2D network," *Hacettepe Journal of Mathematics and Statistics*, vol. 47, no. 1, pp. 9–18, 2018.

[2] M. Karelson, *Molecular Descriptors in QSAR/QSPR*. New York: Wiley, 2000.

[3] R. Todeschini and V. Consonni, *Handbook of Molecular Descriptors*. Weinheim: Wiley-VCH, 2000.

[4] A. Ahmad, "Computation of certain topological properties of honeycomb networks and graphene," *Discrete Mathematics, Algorithms and Applications*, vol. 9, no. 5, pp. 1750064, 2017. https://doi.org/10.1142/S1793830917500641.

[5] Ahmad, K. Elahi, R. Hasni and M. F. Nadeem, "Computing the degree based topological indices of line graph of benzene ring embedded in P-type-surface in 2D network," *Journal of Information and Optimization Sciences*, vol. 40, no. 7, pp. 1511–1528, 2019.

[6] M. Bača, J. Horváthová, M. Mokrišová, A. Semaničová-Feňovčíková and A. Suhányiová, "On topological indices of carbon nanotube network," *Canadian Journal of Chemistry*, vol. 93, no. 10, pp. 1157–1160, 2015.

[7] H. Wiener, "Structural determination of paraffin boiling points," *Journal of the American Chemical Society*, vol. 69, no. 1, pp. 17–20, 1947.

[8] M. Bača, J. Horváthová, M. Mokrišová and A. Suhányiová, "On topological indices of fullerenes," *Applied Mathematics and Computation*, vol. 251, pp. 154–161, 2015.

[9] G. Hong, Z. Gu, M. Javaid, H. M. Awais and M. K. Siddiqui, "Degree-based topological invariants of metal-organic networks," *IEEE Access*, vol. 8, pp. 68288–68300, 2020.

[10] A. Ahmad, "Topological properties of sodium chloride," *Scientific Bulletin-University Politehnica of Bucharest, Series B*, vol. 82, no. 1, pp. 35–46, 2020.

[11] Gutman, J. Tošović, S. Radenković and S. Marković, "On atom-bond connectivity index and its chemical applicability," *Indian Journal of Chemistry*, vol. 51, pp. 690–694, 2012.

[12] M. Javaid, J.-B. Liu, M. A. Rehman and S. Wang, "On the certain topological indices of titania nanotube $TiO_{2[m,n]}$," *Zeitschrift fur Naturforschung A*, vol. 72, no. 7, pp. 647–654, 2017.

[13] S. Zaman, F. A. Abolaban, A. Ahmad and M. A. Asim, "Maximum H-index of bipartite network with some given parameters," *AIMS Mathematics*, vol. 6, no. 5, pp. 5165–5175, 2021.

[14] S. Hayat and M. Imran, "Computation of topological indices of certain networks," *Applied Mathematics and Computation*, vol. 240, pp. 213–228, 2014.

[15] Ali, N. A. Koam and A. Ahmad, "Polynomials of degree-based indices for three-dimensional mesh network," *Computers, Materials and Continua*, vol. 65, no. 2, pp. 1271–1282, 2020.

[16] Ali, N. A. Koam, A. Ahmad and M. F. Nadeem, "Comparative study of valency-based topological descriptor for hexagon star network," *Computer Systems Science and Engineering*, vol. 36, no. 2, pp. 293–306, 2021.

[17] A. Ahmad, R. Hasni, K. Elahi and M. A. Asim, "Polynomials of degree-based indices for swapped networks modeled by optical transpose interconnection system," *IEEE Access*, vol. 8, pp. 214293–214299, 2020.

[18] T. Došlić, B. Furtula, A. Graovac, I. Gutmanb, S. Moradid *et al.,* "On vertex-degree-based molecular structure descriptors," *MATCH Communications in Mathematical and in Computer Chemistry*, vol. 66, pp. 613–626, 2011.

[19] M. Chellali, T. W. Haynes, S. T. Hedetniemi and T. M. Lewis, "On *ve*-degrees and *ev*-degrees in graphs," *Discrete Mathematics*, vol. 340, no. 2, pp. 31–38, 2017.

[20] M. Cancan, "On ev-degree and ve-degree topological properties of tickysim spiking neural network," *Computational Intelligence and Neuroscience*, vol. 2019, pp. 1–7, 2019.

[21] A. Ahmad, "Comparative study of *ve*-degree and *ev*-degree topological descriptors for benzene ring embedded in P-type-surface in 2D network," *Polycyclic Aromatic Compounds*. https://doi.org/10.1080/10406638.2020.1834415.

[22] S. Ediz, "A new tool for QSPR researches: *ev*-degree Randic index," *Celal Bayar Universitesi Fen Bilimleri Dergisi*, vol. 13, no. 3, pp. 615–618, 2017.

[23] S. Ediz, "On *ve*-degree molecular topological properties of silicate and oxygen networks," *International Journal of Computer Science Mathematics*, vol. 9, no. 1, pp. 1–12, 2018.

[24] Horoldagva, K. C. Das and T. A. Selenge, "On *ve*-degree and *ev*-degree of graphs," *Discrete Optimization*, vol. 31, pp. 1–7, 2019.

[25] B. Sahin and S. Ediz, "On *ev*-degree and *ve*-degree topological indices," *Iranian Journal of Mathematical Chemistry*, vol. 9, no. 4, pp. 263–277, 2018.

[26] J. Zhang, M. K. Siddiqui, A. Rauf and M. Ishtiaq, "On *ve*-degree and *ev*-degree based topological properties of single walled titanium dioxide nanotube," *Journal of Cluster Science*, 2020. [Online]. Available: https://dx.doi.org/10.1007/s10876-020-01842-3.

[27] N. Zahra, M. Ibrahim and M. K. Siddiqui, "On topological indices for swapped networks modeled by optical transpose interconnection system," *IEEE Access*, vol. 8, pp. 200091–200099, 2020.

[28] R. Tetzlaff, *Cellular Neural Networks and their Applications*. Singapore: World Scientific, 2002.

[29] L. O. Chua and L. Yang, "Cellular neural networks: Theory," *IEEE Transactions on Circuits and Systems*, vol. 35, no. 10, pp. 1257–1272, 1988.

[30] J. B. Liu, Z. Raza and M. Javaid, "Zagreb connection numbers for cellular neural networks," *Discrete Dynamics in Nature and Society*, vol. 2020, pp. 8, 2020.

[31] J.-B. Liu, Z. Jing, W. Shaohui, M. Javaid and C. Jinde, "On the topological properties of the certain neural networks," *Journal of Artificial Intelligence and Soft Computing Research*, vol. 8, no. 4, pp. 257–268, 2018.

[32] M. Imran, M. K. Siddiqui, A. Q. Baig and W. Khalid, "Topological properties of cellular neural networks," *Journal of Intelligent & Fuzzy Systems*, vol. 37, no. 3, pp. 3605–3614, 2019.

[33] V. Bhambhani and H. G. Tanner, "Topology optimization in cellular neural networks," in *49th IEEE Conf. on Decision and Control*, Atlanta, GA, USA, IEEE, 2010.

[34] F. Ejaz, M. Hussain, H. Almohamedh, K. M. Alhamed, R. Alabdan *et al.,* "Dominating topological analysis and comparison of the cellular neural network," *Mathematical Problems in Engineering*, vol. 2021, Article ID 6613433, 9 pages, 2021. https://doi.org/10.1155/2021/6613433.

[35] A. Ahmad, M. Bača, Y. Bashir and M. K. Siddiqui, "Total edge irregularity strength of strong product of two paths," *ARS Combinatoria*, vol. 106, pp. 449–459, 2012.

[36] D. Ma, "The crossing number of the strong product of two paths," *Australasian Journal of Combinatorics*, vol. 68, no. 1, pp. 35–47, 2017.

[37] A. K. Rizhevsky, I. Sutskever and G. E. Hinton, "Image net classification with deep convolutional neural networks," *Advances in Neural Information Processing Systems*, vol. 2, pp. 1097–1105, 2012.

[38] G. Yanan, C. Xiaoqun, L. Bainian and G. Mei, "Solving partial differential equations using deep learning and physical constraints," *Applied Sciences*, vol. 10, pp. 2076–3417, 2020.

[39] J. Sirignano and K. Spiliopoulos, "A deep learning algorithm for solving partial differential equations," *Journal of Computational Physics*, vol. 375, no. 3, pp. 1339–1364, 2018.

[40] H. Jin, Y. Lian and J. Hua, "Learning facial expressions with 3D mesh convolutional neural network," *ACM Transactions on Intelligent Systems and Technology*, vol. 7, pp. 2157–6904, 2018.

[41] N. Kriegeskorte, "Deep neural networks: A new framework for modeling biological vision and brain information processing," *Annual Review of Vision Science*, vol. 1, no. 1, pp. 417–446, 2015.